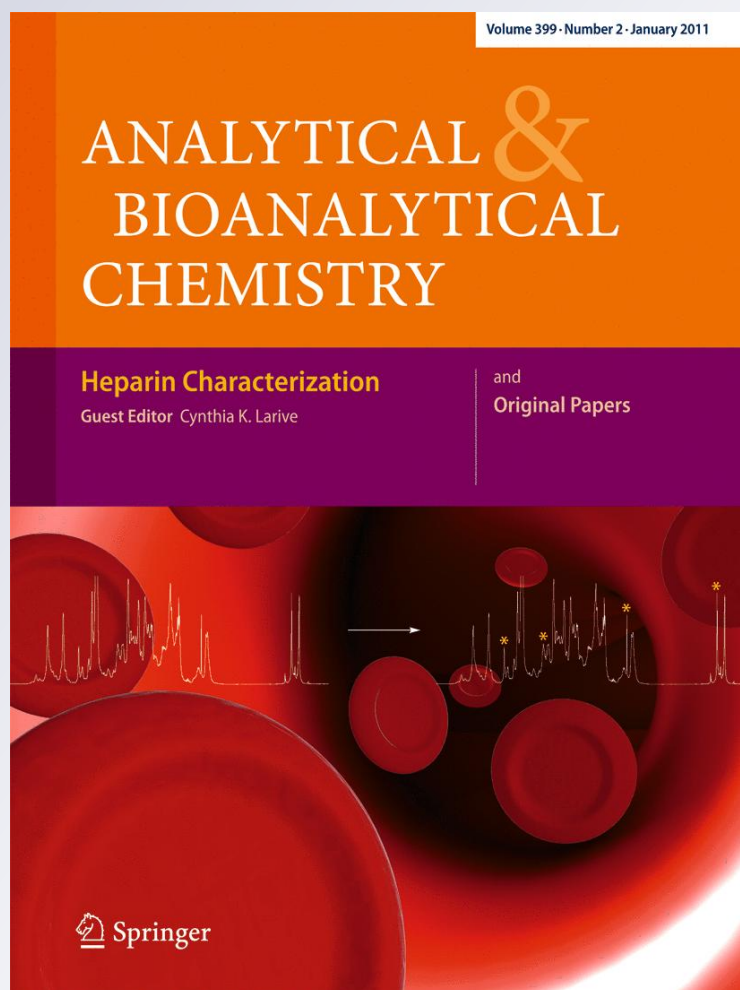


Shotgun lipidomics for candidate biomarkers of urinary phospholipids in prostate cancer

Analytical and Bioanalytical Chemistry

ISSN 1618-2642
Volume 399
Number 2

Anal Bioanal Chem (2010)
399:823-830
DOI 10.1007/
s00216-010-4290-7



Your article is protected by copyright and all rights are held exclusively by Springer-Verlag. This e-offprint is for personal use only and shall not be self-archived in electronic repositories. If you wish to self-archive your work, please use the accepted author's version for posting to your own website or your institution's repository. You may further deposit the accepted author's version on a funder's repository at a funder's request, provided it is not made publicly available until 12 months after publication.

Shotgun lipidomics for candidate biomarkers of urinary phospholipids in prostate cancer

Hye Kyeong Min · Sangsoo Lim · Bong Chul Chung ·
Myeong Hee Moon

Received: 30 August 2010 / Revised: 30 September 2010 / Accepted: 3 October 2010 / Published online: 17 October 2010
© Springer-Verlag 2010

Abstract Qualitative and quantitative profiling of six different categories of urinary phospholipids (PLs) from patients with prostate cancer was performed to develop an analytical method for the discovery of candidate biomarkers by shotgun lipidomics method. Using nanoflow liquid chromatography–electrospray ionization–tandem mass spectrometry, we identified the molecular structures of a total of 70 PL molecules (21 phosphatidylcholines (PCs), 11 phosphatidylethanolamines (PEs), 17 phosphatidylserines (PSs), 11 phosphatidylinositols (PIs), seven phosphatidic acids, and three phosphatidylglycerols) from urine samples of healthy controls and prostate cancer patients by data-dependent collision-induced dissociation. Identified molecules were quantitatively examined by comparing the MS peak areas. From statistical analyses, one PC, one PE, six PSs, and two PIs among the PL species showed significant differences between controls and cancer patients ($p < 0.05$, Student's t test), with concentration changes of more than threefold. Cluster analysis of both control and patient groups showed that 18:0/18:1-PS and 16:0/22:6-PS were 99% similar in upregulation and that the two PSs (18:1/18:0, 18:0/20:5) with two PIs (18:0/18:1 and 16:1/20:2) showed similar (>95%) downregulation. The total amount of each PL group was compared among prostate cancer patients according to the Gleason scale as larger or smaller than 6. It

proposes that the current study can be utilized to sort out possible diagnostic biomarkers of prostate cancer.

Keywords Phospholipids · Quantitative analysis · nLC–ESI–MS/MS · Urine · Prostate cancer · Biomarker

Introduction

Prostate cancer is now the most common lethal male malignancy and the second leading cause of cancer-related death in men in the Western world [1, 2]. Due to the spread of Western-style diets and the aging of the overall population, the incidence of prostate cancer is rapidly increasing worldwide [3]. Clinically, prostate-specific antigen (PSA) levels in blood sera are commonly screened to diagnose prostate cancer, which facilitates early detection [1, 3]. While PSA screening together with digital rectal examination is widely utilized, both the sensitivity and specificity of PSA screening for identifying cancer are relatively low [2]. Studies to discover markers for monitoring prostate cancer using either invasive or noninvasive processes have identified a few proteins. Among these, urinary proteins such as annexin A3 [4], basic human urinary arginine amidase [5], and urinary PSA [6] have been reported as biomarkers. However, even with sophisticated mass spectrometric methods, analysis of target proteins from the urinary proteome remains complicated due to the abundance of proteins in urine. Metabolomic profiling can be used as an alternative approach for developing biomarkers from urine samples. Liquid chromatography–mass spectrometry (LC–MS) has shown that sarcosine levels increase in prostate cancer patients [7], and high-resolution magic angle spinning nuclear magnetic resonance spectroscopy has shown that total levels of phosphocholine and glycerophosphocholine are lowered in prostate cancer

H. K. Min · S. Lim · M. H. Moon (✉)
Department of Chemistry, Yonsei University,
Seoul 120-749, South Korea
e-mail: mhmoon@yonsei.ac.kr

B. C. Chung
Life Sciences Division, Korea Institute of Science
and Technology (KIST),
Seoul 136-791, South Korea

tissue after surgery [8]. Since obtaining a urine sample is easy and noninvasive, biomarkers for detecting prostate cancer are in demand in the metabolomic or lipidomic areas.

Phospholipids (PLs) are major components of cellular membranes and play important roles in cell signaling, proliferation, and death [9, 10]. PLs have complicated molecular types due to the combination of six different polar head groups (choline, ethanolamine, serine, inositol, glycerol, or hydrogen attached to a phosphate group) with various lengths and degrees of unsaturation of the acyl chain. PLs are of increasing interest in lipidomics research because recent studies have shown that they are candidate biomarkers in breast cancer tissue [11–13] and in the plasma of ovarian cancers [14, 15]. Comprehensive qualitative and quantitative analyses of PLs must be accomplished first to develop viable candidate biomarkers for these adult diseases. Recent advances in electrospray ionization–mass spectrometry (ESI–MS) have led to rapid and highly sensitive analyses of PLs [16, 17], but preliminary separation is still required due to the complexity of these molecules. High-performance liquid chromatography (HPLC) coupled to ESI–MS reduces the ionization suppression effect caused by spectral congestion, leading to the enhanced identification of PL species [18–21]. With the help of liquid chromatography–electrospray ionization–tandem mass spectrometry (LC–ESI–MS/MS), PLs can be distinguished by their polar heads and their chain lengths and identified by structures either using a microflow rate [21] or nanoflow rate regime [22, 23], simultaneously lowering the detection limit to 2.2 fmol [24]. Recently, it was demonstrated that 1 mL of human urine can be utilized to extract PLs, yielding 75 different species by nanoflow LC–ESI–MS/MS [25], and further applied for the quantitative analysis of urinary phospholipids from breast cancer patients [26, 27].

In the present study, the shotgun lipidomics method was utilized to investigate urine samples for potential phospholipid markers for prostate cancer. Urinary PL extracts from ten healthy persons and nine prostate cancer patients were qualitatively characterized using nLC–ESI–MS/MS with data-dependent collision-induced dissociation (CID) for structural identification. The two PL groups (phosphatidylcholines (PCs) and phosphatidylethanolamines (PEs)) were analyzed in positive ion mode of nLC–ESI–MS/MS and the other four groups (phosphatidic acids (PAs), phosphatidylinositols (PIs), phosphatidylserines (PSs), and phosphatidylglycerols (PGs)) in negative ion mode. Identified PL molecules were quantitatively analyzed by peak area measurement of nLC–ESI–MS from each individual sample. Statistical analyses indicated that a few PL species exhibited significant differences in relative abundances between control and patient samples. The average concentration of each PL group from patient samples was compared according to the prostate cancer status based on Gleason scales at $G \leq 6$ and $G > 6$.

Experimental

Materials and urine samples

Internal standards were added to PL extract samples at fixed concentrations of 0.5 pmol of 16:0/16:0-PE for the positive ion mode and 0.2 pmol of 14:0/14:0-PG for the negative ion mode, obtained from Avanti Polar Lipids Inc. (Alabaster, AL, USA). The addition of internal standards was to compensate for possible fluctuations in the MS signals of each urine sample during the semiquantitative analysis of each urinary PL species. All solvents used (H_2O , CH_3CN , HCOOH , NH_4OH , $\text{CH}_3\text{CHOHCH}_3$, CH_3OH , and CHCl_3) were of HPLC grade.

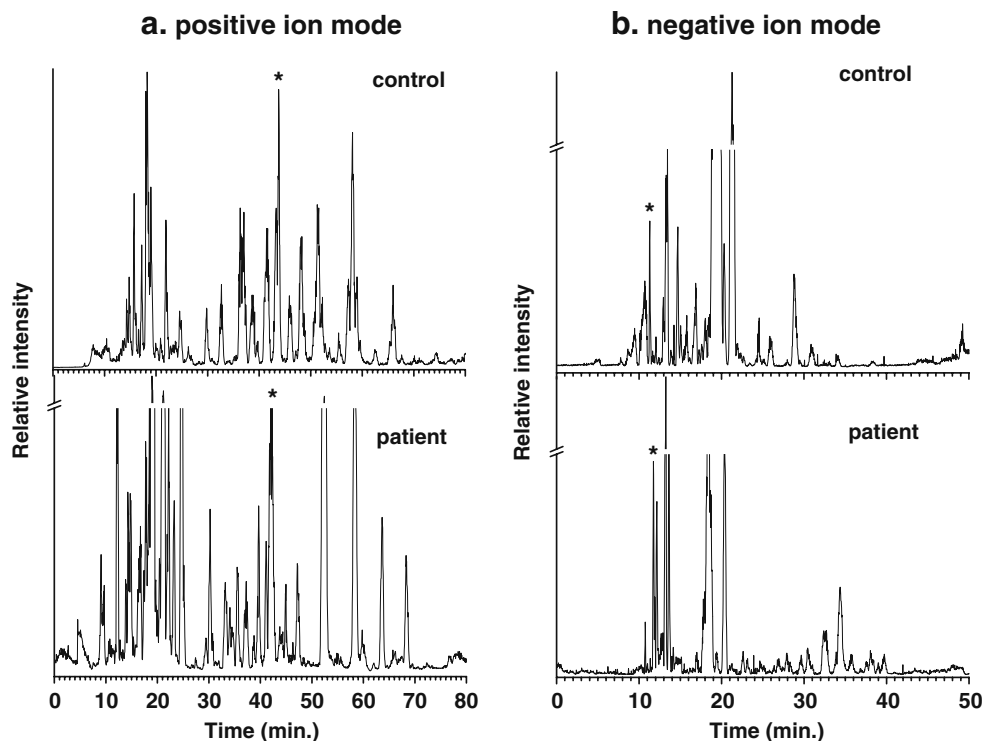
Human urine samples for healthy controls (age range 53–67) and prostate cancer patients (age range 68–83 years) were obtained from Integrated Omics Center, KIST (Seoul, Korea). Patients with prostate cancer were graded using the Gleason scale (or G-scale), the common scale used for grading prostate cancer, with a range of 4–10. The Gleason scale of each patient was provided together with urine sample after a histological examination of patient prostate cells. Extraction of PL species from human urine was done as previously reported [26]. Briefly, 1 mL of each urine sample was lyophilized for 12 h to evaporate the liquid phase; the resulting powder was dispersed with 0.90 mL of 2:1 (v/v) CHCl_3 : CH_3OH by vortexing and then left at room temperature for 1 h. Next, 0.18 mL of H_2O was added, followed by centrifugation at $15,700 \times g$ for 5 min at room temperature. The lower phase containing lipids was recovered and dried using a SpeedVac. The extracted lipid powder was dissolved in $\text{CH}_3\text{OH}/\text{CH}_3\text{CN}$ (1:1) in a final volume of 500 μL and stored at -20°C . For nLC–ESI–MS/MS analysis, this stored lipid solution was diluted to a concentration of 5.0 $\mu\text{g}/\mu\text{L}$ with $\text{CH}_3\text{OH}/\text{CH}_3\text{CN}$ (9:1), and the resulting mixture was injected via autosampler.

For nanoflow LC, 75- μm -i.d. capillary tubes (Polymicro Technology LLC, Phoenix, AZ, USA) were used to create a homemade RPLC column, with 20- and 50- μm -i.d. capillaries for connections (all have 360- μm o.d.). The RPLC column was prepared in our lab by packing reversed-phase resin Magic C_{18} , 5 μm –100 \AA (Michrom Bioresources Inc., Auburn, CA, USA), into 75- μm -i.d. capillary tubing. Before packing, one end of the capillary tube was pulled using a flame to create a sharp needle (tip i.d. $\sim 10 \mu\text{m}$) for direct ESI without an emitter. Then, the pulled tip of the empty column (17 cm) was packed with a methanol slurry of Magic C_{18} , under a constant pressure (1,000 psi) of He.

Nanoflow LC–ESI–MS/MS

A model 1200 capillary pump system from Agilent Technologies (Palo Alto, CA, USA) equipped with an

Fig. 1 Base peak chromatograms of urinary PL extracts from a control and a patient sample obtained by nLC-ESI-MS/MS. Each sample is analyzed at both **a** positive and **b** negative ion mode of analysis for the detection of different PL groups



autosampler was utilized along with the homemade pulled tip capillary column that was directly interfaced to an LCQ Deca XP MAX ion trap mass spectrometer (Thermo Finnigan, San Jose, CA, USA) for nLC-ESI-MS/MS. At the inlet of the capillary column, a PEEK microcross (Upchurch Scientific, Oak Harbor, WA, USA) was connected; the other three connections were used for pump flow, a Pt wire for ESI voltage, and a capillary tube (20 μm i.d., 360 μm o.d.) for venting the split flow, which was

controlled by an on-off valve at the end. This on-off valve was set to be off during sample loading at a pump flow rate of 300 nL/min for 10 min. After sample loading, the gradient elution began at a flow rate of 7 $\mu\text{L}/\text{min}$ with the on-off valve on so that only 300 nL/min of flow was delivered to the analytical column for separation. This was to minimize the dwell time during gradient elution. Mobile-phase solutions for gradient elution were 50/50 (v/v) $\text{CH}_3\text{CN}/\text{dH}_2\text{O}$ for A and 90/10 isopropanol/ CH_3CN for B.

Fig. 2 a MS spectra at 12.76 min (the top BPC of Fig. 1b) during nLC-ESI-MS of a control sample at negative ion mode showing two prominent ions and **b** the data-dependent MS/MS spectra of the ion $m/z=760.8$ representing characteristic fragment ions to support for the identification of 16:0/18:1-PS

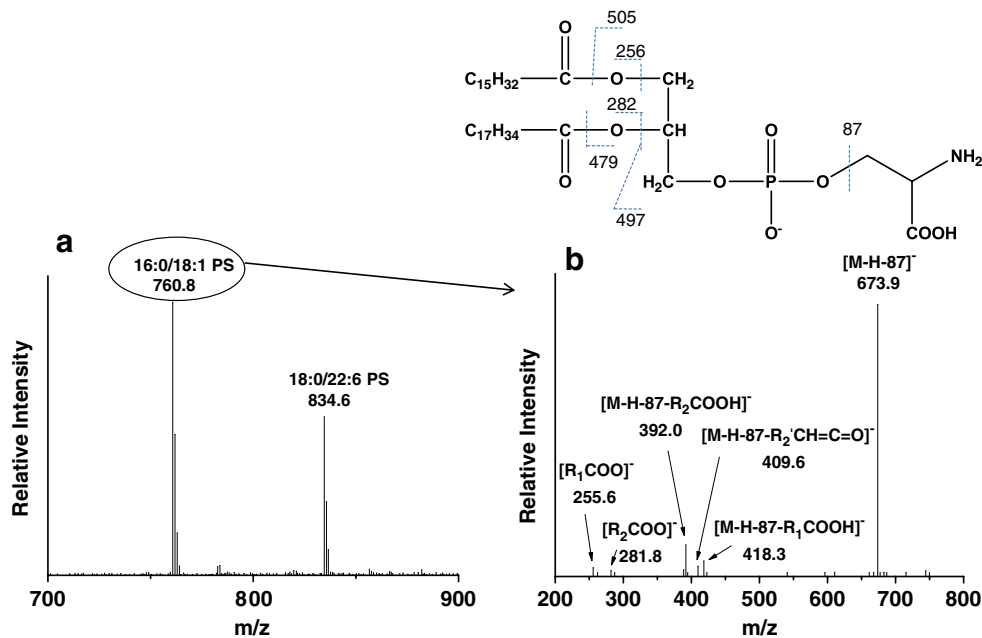


Table 1 Identified urinary PL species from control and patient samples by nLC–ESI–MS/MS along with *p* values from *t* tests and with the relative ratio of peak area between patient and control groups

Class	Molecular species	<i>m/z</i>	Control (<i>n</i> =10)	Patient (<i>n</i> =9)	<i>p</i> value	Ratio	
Positive ion mode							
PC	18:3/18:3	778.9	0.27±0.07	0.50±0.28	0.02	1.83	
	18:3/20:5	802.9	0.37±0.06	0.57±0.16	0.00	1.53	
	18:3/18:4	776.8	0.49±0.12	0.76±0.31	0.02	1.55	
	18:2/14:3	724.6	0.12±0.05	0.13±0.05	0.30	1.10	
	18:2/18:2	782.5	0.03±0.01	0.04±0.02	0.05	1.45	
	18:2/14:2	725.9	0.03±0.01	0.04±0.01	0.01	1.67	
	16:1/16:0	732.9	0.05±0.02	0.03±0.01	0.01	0.69	
	16:0/20:5	781.4	0.07±0.01	0.05±0.01	0.00	0.71	
	16:0/20:4	782.5	0.09±0.02	0.06±0.02	0.02	0.73	
	16:0/18:2	759.1	0.10±0.02	0.56±0.15	0.00	5.52	
	18:2/18:1	784.9	0.03±0.01	0.03±0.01	0.26	1.11	
	16:3/18:5	747.1	0.13±0.05	0.09±0.02	0.02	0.69	
	16:0/16:0	734.8	0.29±0.19	0.10±0.03	0.01	0.36	
	16:0/18:1	760.8	1.04±0.22	0.73±0.13	0.00	0.70	
	18:1/18:1	786.2	0.03±0.01	0.17±0.04	0.00	5.12	
	18:0/18:1	788.8	0.02±0.004	0.08±0.04	0.00	3.26	
	20:3/18:2	809.1	0.002±0.001	0.02±0.003	0.00	13.24	
	14:1/20:4	752.6	0.16±0.04	0.17±0.01	0.29	1.04	
	18:0/20:4	810.8	ND	0.16±0.08	0.00	inf.	
	20:3/18:0	811.7	0.04±0.02	0.08±0.02	0.00	2.34	
	16:1/22:1	815.6	0.37±0.10	0.61±0.07	0.00	1.64	
	PE	18:2/20:4	765.1	0.22±0.05	0.05±0.01	0.00	0.24
		16:4/22:4	759.9	0.08±0.02	0.38±0.08	0.00	4.83
18:2/18:2		741.0	0.05±0.01	0.15±0.04	0.00	2.91	
18:1/20:4		766.6	0.07±0.01	0.04±0.01	0.00	0.62	
16:0/18:2		716.6	0.18±0.03	0.27±0.09	0.01	1.50	
16:0/20:4		740.9	0.25±0.03	0.27±0.04	0.07	1.10	
18:1/18:1		744.6	0.09±0.01	0.17±0.02	0.00	1.97	
16:0/18:1		719.2	0.19±0.03	0.08±0.01	0.00	0.42	
20:1/18:2		770.6	0.08±0.01	0.04±0.01	0.00	0.49	
20:4/18:0		769.5	0.06±0.02	0.08±0.02	0.00	1.45	
20:1/16:0		747.3	0.07±0.02	0.32±0.09	0.00	4.49	
Negative ion mode							
PS	18:0/20:5	808.7	3.34±0.96	0.01±0.07	0.00	0.00	
	18:0/20:4	810.5	2.63±0.62	4.42±3.05	0.12	1.68	
	16:0/22:6	806.6	ND	0.14±0.13	0.01	inf.	
	18:1/22:6	832.9	ND	0.61±0.70	0.03	inf.	
	16:0/18:2	758.8	0.55±0.27	1.03±0.70	0.08	1.88	
	18:1/18:2	784.9	0.10±0.04	0.30±0.52	0.28	2.93	
	16:0/20:4	782.5	0.55±1.27	1.35±0.99	0.14	2.45	
	16:0/18:1	760.6	1.26±0.36	5.28±3.36	0.01	4.20	
	18:1/18:0	788.5	3.46±1.22	0.76±0.55	0.00	0.22	
	18:0/22:6	834.6	0.26±0.25	2.40±1.68	0.01	8.08	
	18:1/18:1	786.7	0.31±0.13	1.80±2.66	0.17	5.27	
	18:2/18:0	786.8	0.41±0.09	0.82±1.99	0.55	2.01	
	18:0/20:3	812.6	0.19±0.04	0.90±0.99	0.06	4.71	
	18:0/22:4	838.7	ND	0.44±0.37	0.01	inf.	

Table 1 (continued)

Class	Molecular species	<i>m/z</i>	Control (<i>n</i> =10)	Patient (<i>n</i> =9)	<i>p</i> value	Ratio
PI	18:0/18:1	788.6	2.24±0.64	36.48±28.06	0.01	16.30
	18:1/20:0	816.8	0.07±0.03	1.12±0.83	0.00	15.38
	22:1/18:1	842.8	0.05±0.05	0.58±4.38	0.72	11.38
	16:0/20:4	857.7	0.99±0.43	0.76±0.48	0.28	0.76
	16:1/20:2	859.6	2.68±1.20	0.52±1.40	0.00	0.19
	16:0/18:1	835.9	0.12±0.03	0.60±1.09	0.27	4.49
	18:6/22:0	909.8	0.11±0.03	0.40±0.37	0.05	3.57
	18:0/20:4	885.5	1.77±0.56	10.54±7.83	0.01	5.97
	18:0/20:3	887.5	0.74±0.26	1.28±2.68	0.56	1.74
	18:0/18:1	863.9	1.94±0.82	0.60±0.25	0.00	0.28
	18:0/18:2	861.9	1.58±0.32	1.20±2.76	0.69	0.76
	20:5/22:1	937.6	4.17±1.63	1.40±1.68	0.00	0.31
	20:2/20:2	913.9	0.52±0.43	0.48±1.19	0.93	0.92
20:2/20:1	915.1	4.91±1.05	8.07±15.08	0.55	1.64	
PG	18:0/14:3	715.7	3.43±0.46	19.43±12.04	0.00	5.66
	20:0/16:2	772.7	2.05±0.91	0.74±0.32	0.00	0.36
	16:2/20:4	766.7	1.80±0.61	0.83±1.00	0.02	0.46
PA	20:4/18:0	723.3	0.91±0.32	1.57±1.91	0.33	1.73
	22:6/18:0	747.1	ND	0.87±0.89	0.02	inf.
	22:6/20:1	772.9	ND	0.72±0.40	0.00	inf.
	20:4/20:1	749.3	4.07±2.16	6.61±3.76	0.09	1.62
	18:1/18:0	701.5	1.32±0.62	0.40±0.27	0.00	0.30
	20:4/20:0	751.5	0.84±0.49	1.06±1.13	0.60	1.27
	18:2/20:0	727.7	1.41±0.74	0.22±0.20	0.00	0.16

Each peak area represents the relative value to the area of the internal standard. Candidate markers are marked in bold characters.

ND not detected, *inf* infinite

To each mobile-phase solution, 0.1% (v/v) formic acid was added for the positive ion mode of nLC–ESI–MS/MS analysis, and 0.05% NH₄OH was added for the negative ion mode. During nLC–ESI–MS/MS analysis of urinary PL extracts, a gradient elution began at 100% mobile phase A, was ramped to 55% mobile phase B over 1 min after sample loading, and then was linearly increased to 90% of B over 90 min for the positive ion mode or over 60 min for the negative ion mode. Injection amounts of urinary lipid extract were 15 µg for the positive ion mode and 5 µg for the negative ion mode. ESI voltages were 2.5 and 3.0 kV for the positive and negative ion modes of analysis, respectively. MS ranges for the precursor scan were *m/z* 660–900 (positive ion mode) and 660–940 (negative ion mode). To achieve CID, the data-dependent MS/MS analysis mode was used for three prominent ions from each precursor scan under 40% (positive) or 45% (negative ion mode) normalized collision energies. Peak areas of each individual PL molecule from the precursor scan of each urine sample were extracted and divided by the peak area of an internal standard. The resulting peak area ratio was used for

comparisons of the control and patient samples. For each sample, three measurements were carried out both for positive and negative ion modes of MS. For statistical treatments, Minitab 15 software (<http://www.minitab.co.kr>) was utilized.

Results and discussion

Identification of PL species from urinary samples

PL mixtures extracted from human urine samples were first analyzed by both positive and negative ion modes of nLC–ESI–MS/MS for the identification of PL molecules. These tests were carried out for all samples including control and prostate cancer patient samples. The base peak chromatograms (BPCs) of one control sample and one patient sample obtained by nLC–ESI–MS/MS (along with the internal standard peak marked with star) are shown in Fig. 1. PCs and PEs were characterized at positive ion mode, and PIs, PAs, PGs, and PSs were characterized at negative ion mode. Structural determination of each molecular species

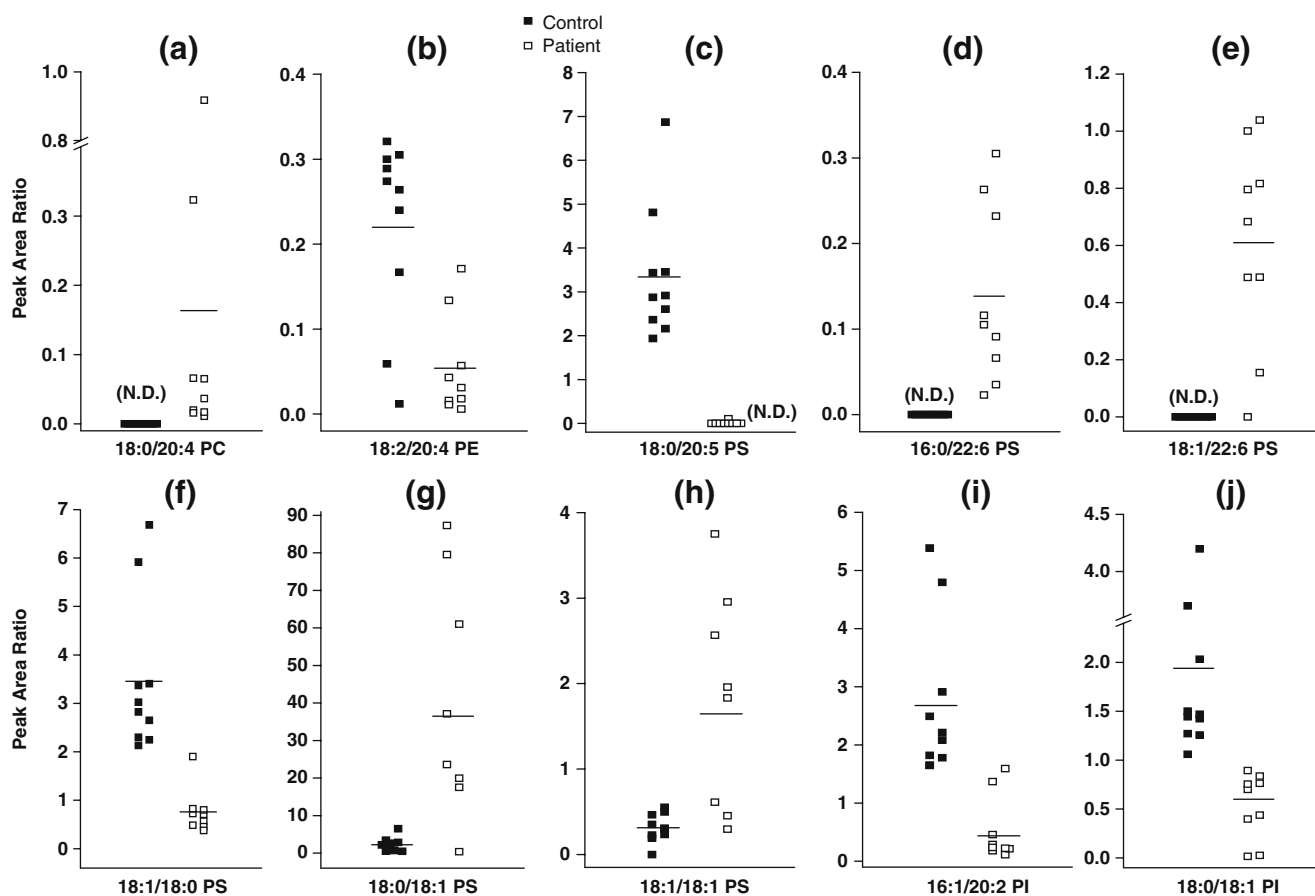


Fig. 3 a–j Relative peak areas (vs. internal standard) of control and patient samples plotted for ten PL species selected from statistical treatments. These ten molecular species represent significant differences ($p < 0.05$) in concentration changes more than threefold in

average and relatively small variation in individual concentrations. The *black squares* represent for control samples, *open squares* represent patients, and each *bar* represents average value

was obtained by the characteristic fragment ion spectra during data-dependent CID. The MS spectra shown (left panel of Fig. 2) are the MS spectrum obtained at a time slice of 12.76 min during nLC separation (Fig. 1b, control sample), showing two prominent ion peaks $[M-H]^-$, at m/z 760.8 and 834.6. The CID spectra of the ions at m/z 760.8 (right panel of Fig. 2) along with ions $[M-H-87]^-$ at m/z 673.9 show a loss of the serine head group ($C_3H_5NO_2$, 87 Da), with fragment ions $[M-H-87-R_1COOH]^-$ and $[M-H-87-R_2COOH]^-$ at m/z 418.2 and 392.0, respectively, representing the loss of each acyl chain as a form of carboxylic acid. The loss of acyl chains as a form of ketene, $[M-H-R_2'CH=C=O]^-$, was seen at m/z 409.6, along with free fatty acid of acyl chains as carboxylate anions, $[R_1COO]^-$ at m/z 255.6 and $[R_2COO]^-$ at m/z 281.8. With the characteristic fragment ions, the CID spectra of the molecular ion m/z 760.8 resulted in the identification of 16:0/18:1-PS, and likewise, the ion m/z 834.6 was found to be 18:0/22:6-PS. A simple example demonstrating how to characterize each PL molecule at

negative ion mode of nLC–ESI–MS/MS is shown in Fig. 2, where 15 μ g of the total lipid extract sample was injected for positive ion mode analysis and 5 μ g was loaded for negative ion mode. Since urinary lipid extracts contain many nonpolar materials including cholesterol, triglycerides, and other lipid molecules, normal injection amounts of urinary lipid extract require a higher amount (three to five times) than tissue samples, as shown in our previous experiments [22, 23]. From qualitative analysis of urinary PLs, 21 PCs and 11 PEs were identified from positive ion mode, and 17 PSs, 11 PIs, seven PAs, and three PGs were identified from negative ion mode of nLC–ESI–MS/MS (Table 1).

Quantitative analysis of PL species between prostate cancer patients and controls

Concentrations of each PL species were examined by comparing the peak area of each ion in an nLC–ESI–MS run. In order to compensate for the fluctuations in MS

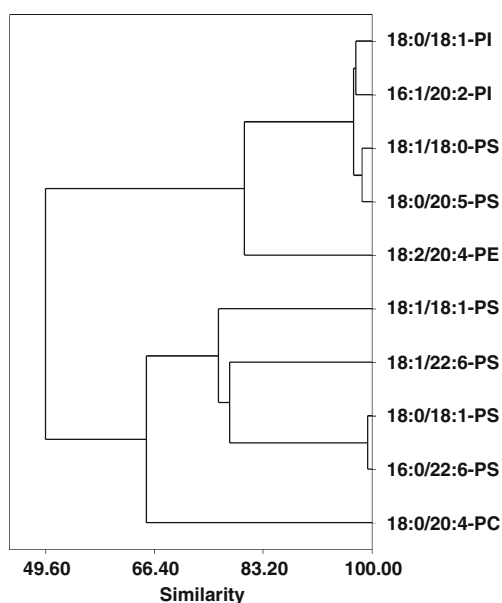


Fig. 4 Cluster analysis dendrogram of similarities using a single linkage method for ten selected PL species

intensities during different runs, peak areas of each individual PL species were divided by that of an internal standard added to each sample; the relative peak area to internal standard is represented in Table 1, with each individual sample being measured in triplicate. The relative peak area represented the average value of the control samples ($n=10$) and of the patients ($n=9$) along with the standard deviation values, p values of the t test accomplished for the control and patient samples, and the ratio of the average peak area values (patient vs. control). For PCs and PEs, the molecular species that showed significant differences by t test ($p<0.05$) as well as those with changes in concentration of more than threefold were 16:0/18:2-PC, 18:1/18:1-PC, 18:0/18:1-PC, 20:3/18:2-PC, 18:0/20:4-PC, 18:2/20:4-PE, 16:4/22:4-PE, and 20:1/16:0-PE. While these species showed significant differences between control and patient samples, the concentration distribution among each group of samples (controls or patients) exhibited a broad variation in some cases. Among these species, few species were selected for concentration distribution plot in Fig. 3 in which individual data points showed a clustered result in any group of sample. For instance, 18:0/20:4-PC was selected because it was not detected at all in the control samples, but it did appear in patient samples with relatively clustered data points for patient group except two outlying values in concentration range (Fig. 3a). The concentration of 18:2/20:4-PE in the patient group resulted in a fourfold of decrease with some clustering in concentration distribution (Fig. 3b).

Among the PLs detected in the negative ion mode of nLC-ESI-MS/MS, nine PSs, six PIs, one PG, and four PAs

show significant differences between the control and patient groups by t test ($p<0.05$) with more than a threefold concentration change. Among these species, eight molecules showing clustered data points either from the control group or the patient group were plotted (Fig. 3c-j). One species, 18:0/20:5-PS, was detected in only one patient sample and showed a clear difference from the control sample in a concentration distribution plot (Fig. 3). While 16:0/22:6-PS and 18:1/22:6-PS were detected only in patient samples, the concentration scales of these two species in the patient group was very small compared with the changes observed in 18:0/20:5-PS (Fig. 3d-e). However, 18:1/18:0-PS (Fig. 3f) showed a distinct decrease in concentration with clustered data points (narrow concentration distribution) for the patient group, while its regioisomer, 18:0/18:1-PS (Fig. 3g), exhibited a narrow distribution for the control group but showed a large increase in concentration (16.30-fold) in the patient group with a broad distribution. The relative peak area of 18:0/18:1-PS is the largest among the PS molecules and all other ions detected in the negative ion mode of nLC-ESI-MS/MS. Characterization of the 18:0/18:1-PS regioisomers by nLC-ESI-MS/MS demonstrated opposite trends in concentration change for the prostate cancer patient group as compared with the control group; these data could be a merit of employing nLC separation of PL extracts. The 18:1/18:1-PS species also showed an increase similar to 18:0/18:1-PS but with less change in concentration scale (Fig. 3h). It was also noted that concentration levels of 16:1/20:2-PI and 18:0/18:1-PI (Fig. 3i-j) were significantly decreased.

A hierarchical cluster analysis using the single linkage method was carried out for the ten PL species selected to detect correlations among individual PL species (Fig. 3). The resulting dendrogram is plotted in Fig. 4. Among the ten PL species, 18:0/18:1-PS and 16:0/22:6-PS are ~99% similar (a simultaneous increase can be seen in Fig. 3). Secondly, 18:1/18:0-PS and 18:0/20:5-PS exceed 97%

Table 2 Comparison of average peak area of each PL category for prostate cancer patient groups according to Gleason scales

	Average peak area (per person)		Ratio
	G \leq 6 ($n=4$)	G $>$ 6 ($n=5$)	
PCs	2.03 \pm 0.09	7.35 \pm 0.27	3.62
PEs	0.75 \pm 0.04	2.74 \pm 0.15	3.65
PSs	31.42 \pm 7.30	79.29 \pm 11.24	2.52
PIs	24.79 \pm 7.22	6.60 \pm 4.53	0.27
PGs	35.98 \pm 5.70	2.47 \pm 4.81	0.07
PAs	17.70 \pm 1.68	3.83 \pm 2.24	0.22

similarity, and 18:0/18:1-PI and 16:1/20:2-PI are above 96%. These two pairs exhibit over 95% similarity, and all show a decrease in concentration for the patient group. However, a concentration increase in 18:0/20:4-PC is not strongly correlated in the four PS species, which showed an increase pattern in the patient group (Fig. 3).

The total amount of each PL group was compared among prostate cancer patients according to the Gleason scale rating of larger or smaller than 6. The average peak area of each PL category for $G \leq 6$ per patient ($n=4$ patients) was compared with that for $G > 6$ ($n=5$) (Table 2). We found that the average amount of each PC, PE, and PS group increased by 2.5–3.6-fold in patients having G scales larger than 6, and the amount of each PI, PG, and PA group decreased more than fourfold. Though the number of patient samples examined is not large enough to predict a certain trend in this study, this result shows that the PL molecular distribution changes critically upon the development of prostate cancer.

Conclusions

Our results demonstrate that nLC–ESI–MS/MS along with statistical analysis can be utilized to distinguish PL species with significantly different concentrations from normal in urine samples to patients with prostate cancer. Although the present work is preliminary with a limited number of samples (19 samples), it provides a guideline to screen potential markers that, in the future, could be used as target molecules for high-speed scanning of a large number of samples. From this study, ten PL species are proposed as possible target molecules. Species showing significant differences in patient samples as well as those with similarities among species from cluster analysis are 18:0/18:1-PS and 16:0/22:6-PS for upregulated cases and 18:1/18:0-PS, 18:0/20:5-PS, 18:0/18:1-PI, and 16:1/20:2-PI for downregulated cases. For cases of PL species showing increases for the patient group, variations in individual concentrations appear to be relatively large. However, for those showing decreases in concentration, observed concentration variations for patient samples were small. Two PS molecules (18:1/18:0-PS and 18:0/20:5-PS) showed clear decreases in concentration distribution for the patient group. While the current study suggests candidate biomarkers for prostate cancer, there is a possible deviation arising from the difference in the age groups between healthy and patient samples. For the confirmation of urinary PL biomarkers for prostate cancer, a systematic examination of the proposed PL markers with a larger number of patient samples are expected.

Acknowledgements This study was supported by grant NRF-2008-2003136 and in part by grant NRF-2010-0014046 from the National Research Foundation of Korea.

References

- Gronberg H (2003) *Lancet* 163:859–864
- Clarke RA, Schirra HJ, Catto JW, Lavin MF, Gardiner RA (2010) *Cancer* 2:1125–1154
- Hsing AW, Devesa SS (2001) *Epidemiol Rev* 23:3–13
- Gerke V, Creutz CE, Moss SE (2005) *Nat Rev Mol Cell Biol* 6:449–461
- Matsuda Y, Miyashita A, Fujimoto Y, Umeda T, Akihama S (1996) *Biol Pharm Bull* 19:1083–1085
- Irani J, Salomon L, Soulié M, Zlotta A, de la Taille A, Dore B, Millet C (2005) *Urology* 65:533–537
- Sreekumar A, Poisson LM, Rajendiran TM, Khan AP, Cao Q, Yu J, Laxman B, Mehra R, Lonigro RJ, Li Y, Nyati MK, Ahsan A, Kalyana-Sundaram S, Han B, Cao X, Byun J, Omenn GS, Ghosh D, Pennathur S, Alexander DC, Berger A, Shuster JR, Wei JT, Varambally S, Beecher C, Chinnaiyan AM (2009) *Nature* 457:910–914
- Swanson MG, Vigneron DB, Tabatabai ZL, Males RG, Schmitt L, Carroll PR, James JK, Hurd RE, Kurhanewicz J (2003) *Magn Reson Med* 50:944–954
- Brouwers JFHM, Vernooji EAAM, Tielens AGM, van Golde LMG (1999) *J Lipid Res* 40:164–169
- Wright MM, Howe AG, Zaremborg V (2004) *Biochem Cell Biol* 82:18–26
- Leach MO, Verrill M, Glaholm J, Smith TAD, Collins DJ, Payne GS, Sharp JC, Ronen SM, McCreedy VR, Powles TJ, Smith IE (1998) *NMR Biomed* 11:314–340
- Williams CM, Maunder K (1993) *Eur J Clin Nutr* 47:260–267
- Bougnoux P, Chajes V, Lanson M, Hacene K, Body G, Couet C, Folch OL (1992) *Breast Cancer Res Treat* 20:185–194
- Xu Y, Shen Z, Wiper DW, Wu M, Morton RE, Elson P, Kennedy AW, Belinson J, Markman M, Casey G (1998) *JAMA* 280:719–723
- Sutphen R, Xu Y, Wilbanks GD, Fiorica J, Grendys EC Jr, LaPolla JP, Arango H, Hoffman MS, Martino M, Wakeley K, Griffin D, Blanco RW, Cantor AB, Xiao YJ, Krischer JP (2004) *Cancer Epidemiol Biomark Prev* 13:1185–1191
- Han X, Gross RW (1995) *J Am Soc Mass Spectrom* 6:1202–1210
- Koivusalo M, Haimi P, Heikinheimo L, Kostianen R, Somerharju P (2001) *J Lipid Res* 42:663–672
- Taguchi R, Hayakawa J, Takeuchi Y, Ishida M (2000) *J Mass Spectrom* 35:953–966
- Isaac G, Bylund D, Mansson J-E, Markides KE, Bergquist J (2003) *J Neurosci Methods* 128:111–119
- Hermansson M, Uphoff A, Käkälä R, Somerharju P (2005) *Anal Chem* 77:2166–2175
- Taguchi R, Houjou T, Nakanishi H, Yamazaki T, Ishida M, Imagawa M, Shimizu T (2005) *J Chromatogr B* 823:26–36
- Bang DY, Kang D, Moon MH (2006) *J Chromatogr A* 1104:222–229
- Bang DY, Ahn E, Moon MH (2007) *J Chromatogr B* 852:268–277
- Ahn E, Kim H, Chung BC, Moon MH (2007) *J Sep Sci* 30:2598–2604
- Kim H, Ahn E, Moon MH (2008) *Analyst* 133:1656–1663
- Kim H, Min HK, Kong G, Moon MH (2009) *Anal Bioanal Chem* 393:1649–1656
- Min HK, Kong G, Moon MH (2010) *Anal Bioanal Chem* 396:1273–1280